Check for updates

A Journal of the Gesellschaft Deutscher Chemiker

Angewandte International Edition GDCh Chemie

www.angewandte.org

Accepted Article

Title: Phototransposition of Indazoles to Benzimidazoles: Tautomer-Dependent Reactivity, Wavelength Dependence, and Continuous Flow Studies

Authors: G. Logan Bartholomew, Sojung F. Kim, Yusuke Oyamada, Federica Sbordone, Joshua A. Carroll, Justin E. Jurczyk, Charles S. Yeung, Christopher Barner-Kowollik, and Richmond Sarpong

This manuscript has been accepted after peer review and appears as an Accepted Article online prior to editing, proofing, and formal publication of the final Version of Record (VoR). The VoR will be published online in Early View as soon as possible and may be different to this Accepted Article as a result of editing. Readers should obtain the VoR from the journal website shown below when it is published to ensure accuracy of information. The authors are responsible for the content of this Accepted Article.

To be cited as: *Angew. Chem. Int. Ed.* **2025**, e202423803

Link to VoR: https://doi.org/10.1002/anie.202423803

WILEY VCH

10.1002/anie.202423803

WILEY VCH

RESEARCH ARTICLE

Phototransposition of Indazoles to Benzimidazoles: Tautomer-Dependent Reactivity, Wavelength Dependence, and Continuous Flow Studies

G. Logan Bartholomew[a], Sojung F. Kim[a]†, Yusuke Oyamada[a]†, Federica Sbordone[b], Joshua A. Carroll[b], Justin E. Jurczyk[c], Charles S. Yeung*[d], Christopher Barner-Kowollik*[b,e,f], Richmond Sarpong*[a]

†These authors contributed equally.

[a] Dr. G. L. Bartholomew, S. F. Kim, Y. Oyamada, Prof. Dr. R. Sarpong
Department of Chemistry
University of California, Berkeley
Berkeley, California, 94720, United States
E-mail: rsarpong@berkeley.edu

[b] F. Sbordone, J. Carroll, Prof. Dr. C. Barner-Kowollik
School of Chemistry and Physics, Centre for Materials Science
Queensland University of Technology (QUT)
Brisbane, Queensland, 4000, Australia
E-Mail: christopher.barnerkowollik@qut.edu.au

[c] Dr. J. E. Jurczyk
Process Chemistry
Gilead Sciences, Inc.
Foster City, California, 94404, United States

[d] Dr. C. S. Yeung
Discovery Chemistry
Merck & Co., Inc.
Boston, Massachusetts, 02115, United States
E-Mail: charles.yeung@merck.com

[e] Prof. Dr. C. Barner-Kowollik
Institute of Nanotechnology (INT), Karlsruhe Institute of Technology (KIT)
Kaiserstrasse 12, 76131 Karlsruhe, Germany
E-Mail: christopher.barner-kowollik@kit.edu

[f] Prof. Dr. C. Barner-Kowollik
Institute of Functional Interfaces (IFG), Karlsruhe Institute of Technology (KIT)
Kaiserstrasse 12, 76131 Karlsruhe, Germany
E-Mail: christopher.barner-kowollik@kit.edu

Supporting information for this article is given via a link at the end of the document.

Abstract: Herein, we report a detailed investigation of the photomediated transformation of indazoles to benzimidazoles through a nitrogen-carbon transposition. This phototransposition is known to occur in low yield when 1H-indazoles are subjected to high-energy UVC irradiation. The 2H-tautomer of indazole absorbs light more strongly than the 1H-tautomer at longer wavelengths. We leveraged this improved absorbance profile to develop a general system for the high-yielding conversion of N2-derivatized indazoles (prepared from the corresponding 1H-indazoles) to the corresponding benzimidazoles under UVB or UVA irradiation in up to 98% yield. Investigation of the substrate scope revealed a strong correlation between reaction yield and electron density at N2 of the indazole substrate, suggesting the importance of the availability of the lone pair at this position for reaction efficiency. In addition, evaluation of wavelength-dependent reactivity through the generation of a photochemical action plot revealed that the highest conversion does not only occur at the substrate's maximum absorbance wavelength but also on its red-side, enabling the use of longer wavelength irradiation to achieve high yields. Building on these insights, a continuous flow protocol was established that enables the phototransposition on preparative scale.

Introduction

The transformative impact of late-stage small molecule diversification on pharmaceutical discovery campaigns has recently led to an intense focus on developing reactions that

This article is protected by copyright. All rights reserved.

15213773, ja, Downloaded from https://onlinelibrary.wiley.com/doi/10.1002/anie.202423803 by Univ of California Lawrence Berkeley National Lab, Wiley Online Library on [02/03/2025]. See the Terms and Conditions (https://onlinelibrary.wiley.com/terms-and-conditions) on Wiley Online Library for rules of use; OA articles are governed by the applicable Creative Commons License

Accepted Manuscript

10.1002/anie.202423803

WILEY VCH

RESEARCH ARTICLE

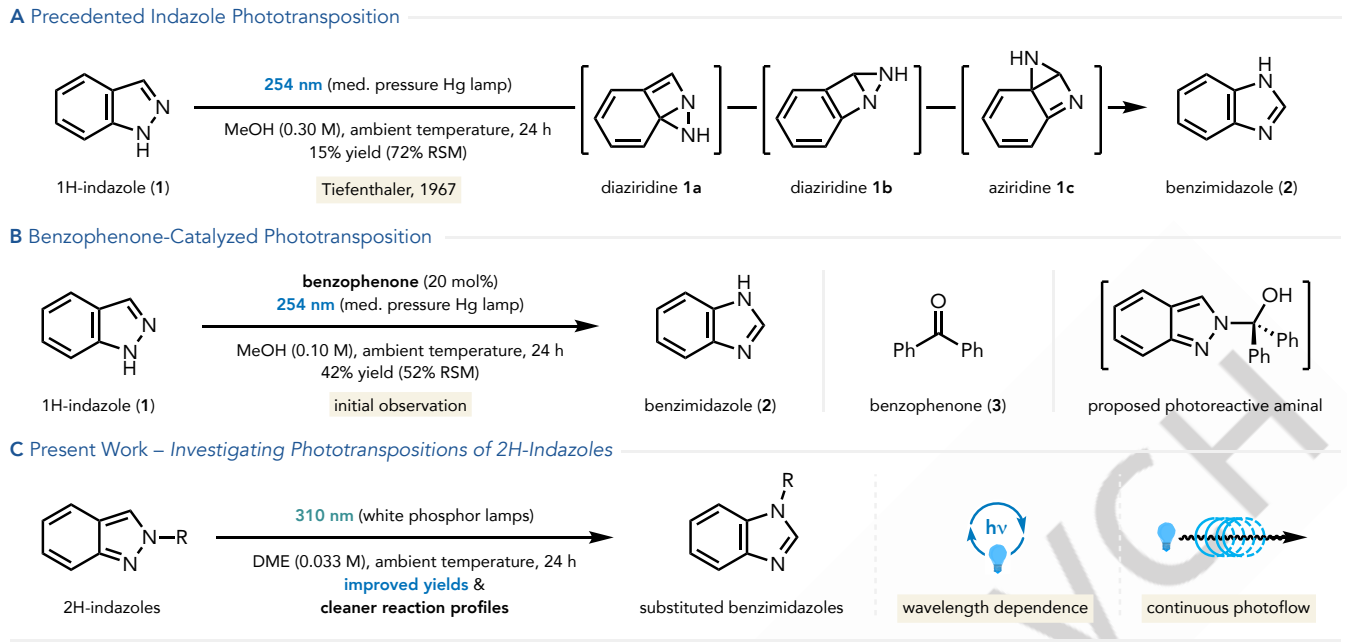

Figure 1. (a) Precedented conditions and a plausible mechanism for photomediated indazole nitrogen atom transposition; (b) Our initial observations of improved transposition yield in the presence of substoichiometric quantities of benzophenone; (c) Schematic summary of the present disclosure.

accomplish "single-atom skeletal edits" of nitrogen heterocycles.[1] Single-atom skeletal edits[2] of heteroaromatic groups can provide novel opportunities to exploit the reactivity of one heterocycle series (e.g., the ability of azines to direct C–H functionalization) before its conversion to another class of heterocycles (e.g., azoles).[3] However, much of the early focus of skeletal editing has been on transformations that accomplish *topological* changes in converting one heterocyclic series to another (e.g., through ring expansions or contractions). Alternatively, *transmutative* skeletal editing, where one atom type is replaced by another, or two atoms have swapped positions, retains the overall shape of the molecule while potentially presenting different exit vectors. Transmutative skeletal edits are currently underrepresented in the rapidly growing synthetic toolbox of skeletal editing reactions. As such, the development of general methods for transmutative skeletal editing should significantly expand core-atom diversification strategies, particularly for pharmaceutically relevant heteroaromatics, by providing a complement to transformations that accomplish topological changes.

Recently, many skeletal editing transformations of heteroarenes have been reported.[3–18] A number of powerful photomediated skeletal edits of both saturated and aromatic nitrogen heterocycles have also emerged.[12,19–22] Of note, the photochemistry of aromatic azoles and related heteroarenes has been studied for over half a century.[23–25] In 1967, Messer et al. reported the conversion of a pyrazole to an imidazole under UVC (200–280 nm) irradiation.[26] In the same year, Tiefenthaler et al. reported an expanded study on the phototransposition of carbon and nitrogen atoms in azoles under similar conditions.[27] Unfortunately, these reactions proceeded in low yield and with narrow reported substrate scopes. Since these early studies, the photomediated conversion of indazoles to benzimidazoles has been intermittently explored by various research groups,[28–30] yet the underlying mechanism remains unresolved.[31,32] Several related five-membered heteroarenes are also known to undergo analogous C–X transposition reactions upon exposure to UVC (100–280 nm) or UVB (280–315 nm) light.[15,33–42] In some cases, the initial photoproducts of these reactions can be intercepted and characterized,[42,43] and a continuous flow protocol has been developed for the conversion of isoxazoles to oxazoles.[44]

We have studied the indazole to benzimidazole transformation in detail across an expanded scope of substrates to improve synthetic utility and also interrogated previously unexplored wavelength-dependent reactivity. Our initial studies focused on 1H-indazoles. Irradiating a solution of 1H-indazole (**1**) in methanol with UVC light centered at 254 nm led to expectedly low conversions, whereas modest increases in yield occurred when substoichiometric quantities of benzophenone were added. While benzophenone is a known triplet sensitizer, it has a similar triplet energy (E_T = 69 kcal/mol)[45] to both 1H- and 2H-indazole (E_T = 67–68 kcal/mol)[46], which precludes efficient triplet sensitization. Instead, we postulated that excited-state benzophenone may "trap" the 2H-tautomer of indazole (Figure 1B, right), N2-alkylated variants of which are known to be more photoreactive.[47,48] We leveraged this recognition to develop a longer-wavelength UVB-mediated conversion of *N*-alkyl 2H-indazoles to benzimidazoles. Recognition of the photoreactive tautomer provided an opportunity to more directly study the efficiency of this reaction using a photochemical action plot. Photochemical action plots, although seldom employed to study organic photochemical transformations, are a powerful technique that provide insight into the wavelength-dependent efficiency of photochemical reactions. Here, the indazole-to-benzimidazole conversion provides another opportunity to expand our understanding of photochemical organic transformations, and the identified optimal wavelength was important in realizing the phototransposition on preparative scale in continuous flow.

Results and Discussion

This article is protected by copyright. All rights reserved.

15213773, ja, Downloaded from https://onlinelibrary.wiley.com/doi/10.1002/anie.202423803 by Univ of California Lawrence Berkeley National Lab, Wiley Online Library on [02/03/2025]. See the Terms and Conditions (https://onlinelibrary.wiley.com/terms-and-conditions) on Wiley Online Library for rules of use; OA articles are governed by the applicable Creative Commons License

Accepted Manuscript

10.1002/anie.202423803

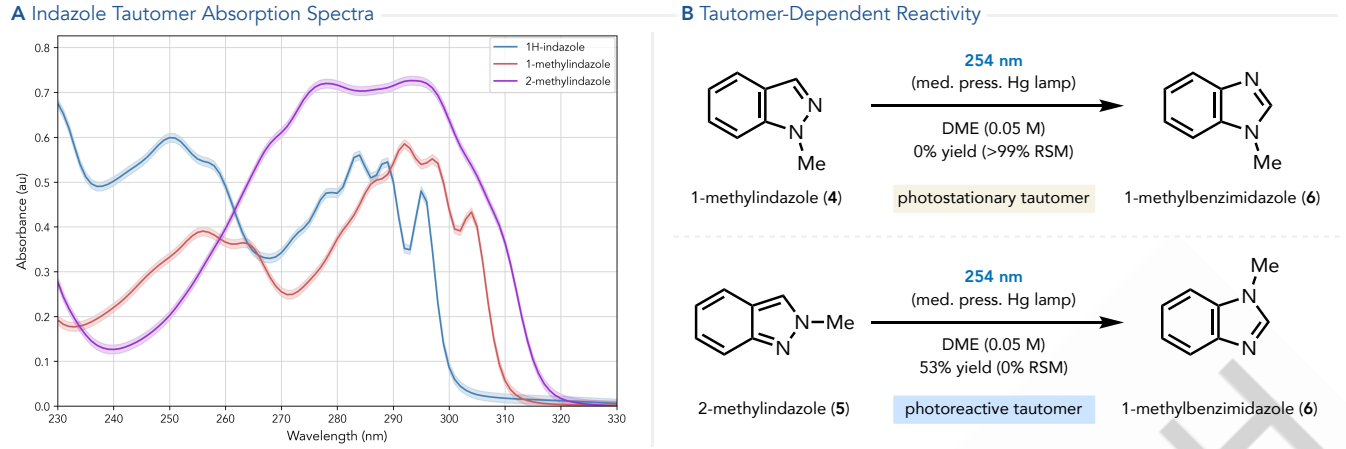

C Effect of Solvent and Concentration on Indazole Phototransposition

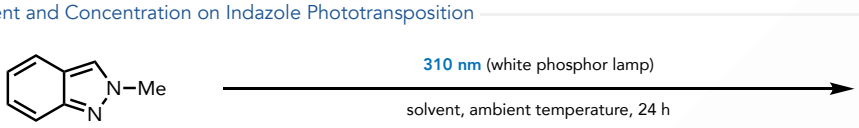

entry	solvent	concentration (M)	yield (%)[a]	RSM (%)
1	DME	0.10	76	24
2	PhMe	0.10	52	32
3	PhH	0.10	62	24
4	DCM	0.10	63	22
5	MeCN	0.10	80	12
6	MeOH	0.10	48	32
7	DME	0.05	84	9
8	DME	0.033	98	0
9[b]	**DME**	**0.033**	**88**	**0**
10[c]	DME	0.033	54	0
11[d]	DME	0.033	71	0
12[e]	DME	0.033	53	0
13[f]	DME	0.033	50	38

Figure 2. (a) UV/Vis absorption spectra of 1H-indazole (blue), 1-methylindazole (red), and 2-methylindazole (violet) at a concentration of 125 μM in acetonitrile; (b) Tautomer-dependent photoreactivity of 1-methylindazole and 2-methylindazole at 254 nm; (c) Improved phototransposition yield at 310 nm (blue) and conditions used for scope evaluation (tan, bold text); solvent, concentration, and condition screening for the photomediated transposition of 2-methyl-2H-indazole. [a]Quantitative 1H NMR yield. [b]Without exclusion of air or trace water. [c]254 nm irradiation. [d]Quartz tube instead of Pyrex. [e]Catalytic quantity of benzophenone (10 mol%) added. [f]Reaction stopped after 12 h.

As reported previously by Tiefenthaler,[27] irradiation of 1H-indazole (**1**) with 254 nm light in 1,2-dimethoxyethane as solvent affords the corresponding benzimidazole (**2**) in 15% yield along with 72% recovered starting material. A plausible mechanism for this transformation, consistent with a proposal by Messer et al.,[26] is shown in Figure 1A. We found that adding 20 mol% of benzophenone (**3**) to the reaction mixture led to a threefold increase in yield to 42%, with 52% of the starting material remaining after irradiating at 254 nm for 24 h. This increase in conversion and yield is likely not due to benzophenone-mediated indazole sensitization,[28] since indazole and benzophenone have similar triplet energies.[45,46] Furthermore, the phototransposition of indazoles to benzimidazoles, as demonstrated by Ferris et al., is known to take place on a singlet energy surface.[28]

Alternatively, we recognized that a key difference existed in the absorption spectra for 1H-indazole (**1**) and its alkylated tautomer, 2-methyl-2H-indazole (**5**). 2-Methyl-2H-indazole (**5**) absorbs more strongly and at longer wavelengths than 1H-indazole (**1**), as shown in the UV-Vis absorption spectra in Figure 2A. We also measured a UV–Vis absorption spectrum for 1-methyl-1H-indazole (**4**; see Figure 2A) with a similar fine structure pattern to that of 1H-indazole, suggesting that protic indazoles exist primarily as the 1H-tautomer in solution.[49] At 90 °C under 254 nm irradiation, 2-methyl-2H-indazole (**5**) is known to convert to the corresponding benzimidazole **6** in much higher yield (93%) than 1H-indazole (**1**) and 1-methyl-1H-indazole (**4**).[27] The low conversion of 1H-indazole (**1**) to the corresponding benzimidazole suggested that the 2H-tautomer of indazole is the species that undergoes productive excitation. The proposed 4π-electrocyclization following excitation[26,30] (see **1** to **1a**) may be more favorable from the 2H-tautomer since the benzenoid portion of the indazole core nominally regains aromaticity in the resulting intermediate (see Figure 1A).

In support of this hypothesis, we found that 1-methylindazole (**4**) is not converted to the corresponding benzimidazole **6** when irradiated at either 254 nm or 310 nm, whereas 2-methylindazole (**5**) is readily transformed at both 254 nm and 310 nm (Figure 2B and 2C). As noted, the transposition of 2-methylindazole (**5**) is known to occur in high yield at elevated temperature with irradiation at 254 nm.[27] We found that **5** undergoes transposition

This article is protected by copyright. All rights reserved.

15213773, ja, Downloaded from https://onlinelibrary.wiley.com/doi/10.1002/anie.202423803 by Univ of California Lawrence Berkeley National Lab, Wiley Online Library on [02/03/2025]. See the Terms and Conditions (https://onlinelibrary.wiley.com/terms-and-conditions) on Wiley Online Library for rules of use; OA articles are governed by the applicable Creative Commons License

Accepted Manuscript

10.1002/anie.202423803

WILEY VCH

RESEARCH ARTICLE

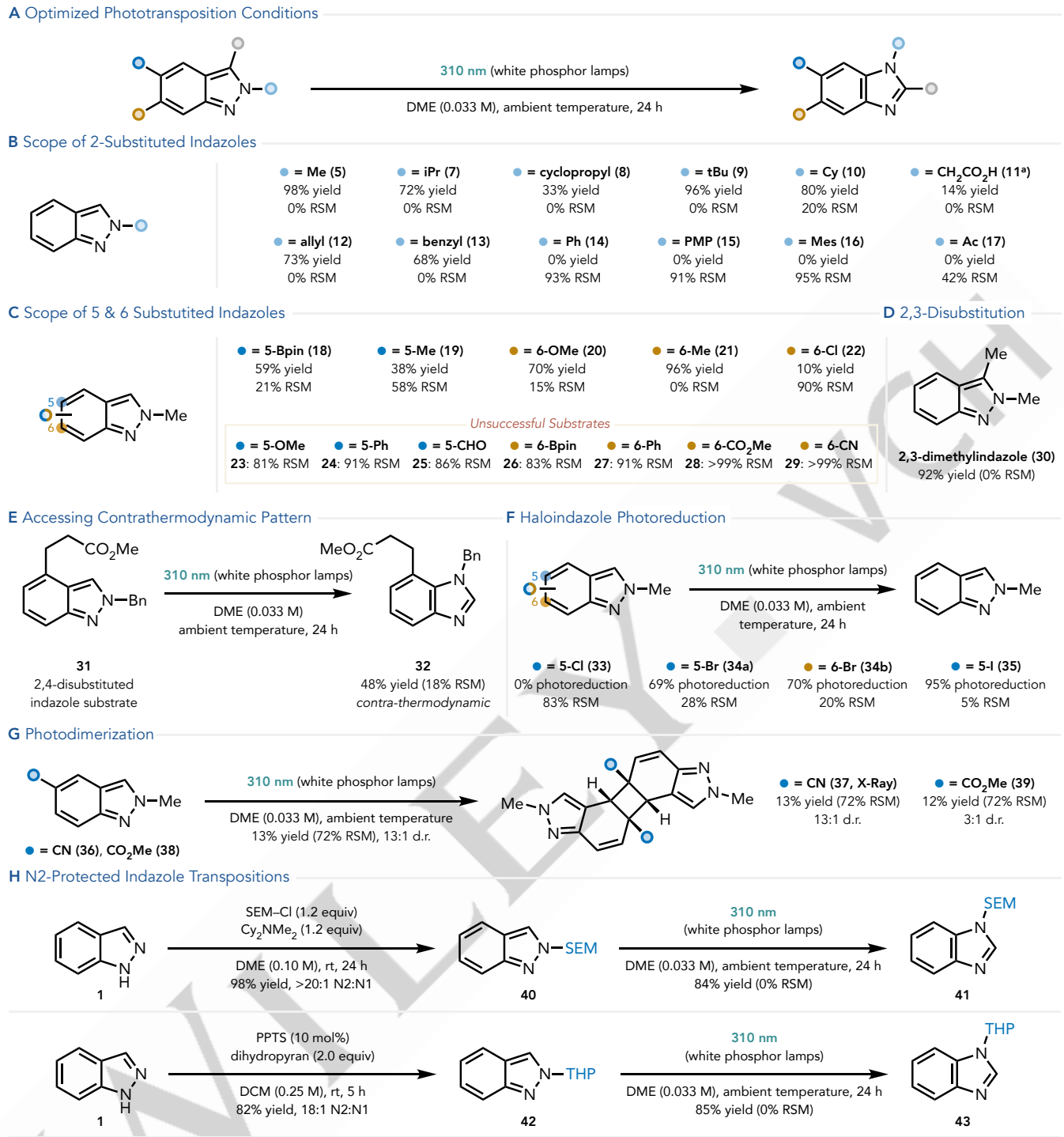

Figure 3. (a) Optimized conditions for scope evaluation without exclusion of air or moisture; (b) Substrate scope of 2-substituted indazoles. [a]Reaction was run in MeOH instead of DME to solubilize the substrate, potentially responsible for reduced yield; (c) Substrate scope of 5- and 6-substituted 2-methylindazoles; (d) Example of a 2,3-disubstituted indazole (3-OMe, 3-Ph, 3-CO_2Me, and 3-CN 2-methylindazoles all gave >90% RSM); (e) Transposition products of a 2,4-disubstituted indazole to give a benzimidazole product with a contra-thermodynamic substitution pattern; (f) Photoreduction of halo-2-methylindazoles. (g) Photodimerization of some 5-substituted 2-methylindazole substrates under the standard conditions; (h) Stepwise and one-pot SEM and THP protection[52–54] and transposition strategies for 1H-indazole.

even at room temperature with 254 nm irradiation, albeit in lower yield (54%). Alternatively, irradiating **5** at 310 nm for 24 h at 25 °C in DME (0.05 M) in a Pyrex tube without stirring afforded methylbenzimidazole **6** in an improved 76% yield along with 24% recovered starting material (Figure 2C, entry 1). Notably, the addition of benzophenone leads to reduced yields of **6** in the conversion of 2-methylindazole (**5**), further suggesting that benzophenone (**3**) is not productively sensitizing the substrate.

With the key recognition that the 2H-tautomer of indazole is likely the photoreactive species, we set out to optimize the reaction conditions using 2-methyl-2H-indazole (**5**), which is easily prepared from 1H-indazole (**1**),[50,51] as a model substrate. Examining the transformation at ambient temperature with irradiation at 310 nm for 24 h using various solvents and concentrations revealed that 1,2-dimethoxyethane (DME) at a concentration of 0.033 M was optimal, enabling the phototransposition of **5** to methylbenzimidazole **6** in 98% yield.

This article is protected by copyright. All rights reserved.

15213773, ja, Downloaded from https://onlinelibrary.wiley.com/doi/10.1002/anie.202423803 by Univ of California Lawrence Berkeley National Lab, Wiley Online Library on [02/03/2025]. See the Terms and Conditions (https://onlinelibrary.wiley.com/terms-and-conditions) on Wiley Online Library for rules of use; OA articles are governed by the applicable Creative Commons License

Accepted Manuscript

10.1002/anie.202423803

RESEARCH ARTICLE

Optimization data are summarized in Figure 2C. The efficiency of the reaction was higher at lower reaction concentrations pointing to the high likelihood of a unimolecular reaction—a slightly diminished yield of 84% with no recovered starting material was obtained when the reaction was conducted at 0.05 M in DME. Yields steadily decreased as reaction concentration increased (see the Supporting Information for details). At the scales and concentrations employed in our studies, stirring was not required and the reaction solutions generally remained homogenous. The reaction profile was much cleaner when the reaction was conducted in a Pyrex tube (which blocks wavelengths shorter than 300 nm) instead of a quartz tube. Additionally, we found that rigorously air- and moisture-free conditions did not significantly improve yields. Therefore, substrates were evaluated without special precautions to exclude air or moisture, which made the setup for these reactions operationally simple.

With optimal conditions for the phototransposition of 2H-indazoles in hand (Figure 2C, entry 9), we investigated the effect of different substituents at N2 of the indazole on reaction efficiency. These results are summarized in Figure 3B. A broad range of alkyl substituents are well-tolerated, including isopropyl, *tert*-butyl, and cyclohexyl, reflecting insensitivity of the reaction to steric encumbrance at N2 (see substrates **7**–**11**). Methanol instead of DME was required to solubilize carboxylic acid **11**, potentially further reducing yield (refer to Figure 2B, entry 6). Substrates with unsaturated substituents at N2 such as 2-allylindazole **12** and 2-benzylindazole **13** also underwent phototransposition in good yields. However, indazoles with directly attached C(sp^2) hybridized groups at N2 (such as substrates **14–17**) did not undergo phototransposition (refer to the Supporting Information for details). These results may reflect the importance of high electron density at N2 of the indazole substrate to the efficiency of the phototransposition.

After evaluating substituents at N2, we investigated the effect of substituents at C3 of the 2-methylindazole model substrate (**5**). Overall, heteroatomic, aryl, and carbonyl substituents at C3 of the indazole are not tolerated, resulting in recovered starting material. However, an alkyl substituent at C3 (see 2,3-dimethylindazole **30**, Figure 3D) underwent the transposition in 92% yield under the typical reaction conditions. Thus, while steric bulk at C3 is tolerated, subtle electronic effects can profoundly influence the photoreactivity of the indazole core.

We next probed the effect of electron-donating and electron-withdrawing substituents at C5 and C6 on the benzenoid portion of 2-methyl-2H-indazole (**5**, Figure 3C). While alkyl groups were well-tolerated (see methylindazoles **19** and **21**), the majority of C5-substituted-2-methylindazoles did not undergo the phototransposition. Of note, boronate ester **18** underwent phototransposition in 59% yield. Interestingly, **18** features an absorption profile similar to that of 2-methylindazole **5**, whereas the absorbances of other C5-substituted indazoles are significantly redshifted relative to that of the model substrate (refer to the Supporting Information for details). However, no productive reactivity occurred using longer wavelength (350 nm) irradiation for these substrates (**23**–**25**) with redshifted absorbance profiles.

Most of the C6-substituted indazoles we investigated also did not undergo phototransposition and returned primarily starting material (Figure 3C). Only 6-methoxyindazole **20** and 6-methylindazole **21** underwent the phototransposition in high yields (70% and 96%, respectively, with 15% recovered starting material for **20**). 6-Chloro-2-methylindazole **22** underwent the transposition in 10% yield with 90% of the starting material recovered.

2,4-Disubstituted indazole **31** underwent phototransposition in 48% yield with 18% starting material recovered to give 1,7-disubstituted benzimidazole **32** (Figure 3E). This result indicates that the phototransposition may be leveraged to access benzimidazole products bearing *contra*-thermodynamic *N*-substitution patterns, which cannot be accessed by *N*-alkylation of the parent benzimidazole.

Halogens that form weak bonds to carbon at C5 and C6 undergo photoreduction (Figure 3F) under our conditions. For example, while 5-chloro-2-methylindazole **33** does not react when irradiated with 310 nm light (83% recovered starting material), 5-bromo-2-methylindazole **34a**, 6-bromo-2-methylindazole **34b**, and 5-iodo-2-methylindazole **35** were converted to 2-methyl-2H-indazole (**5**) in 69%, 70%, and 95% yield, respectively. A plausible mechanism for photoreduction is presented in the Supporting Information. Overall, this data further points to small electronic perturbations having profound effects on the efficiency of the reaction.

Some 2-methylindazoles bearing π electron-withdrawing substituents at C5 underwent an anomalous photomediated [2+2] cycloaddition (Figure 3G). For example, 5-cyanoindazole **36** undergoes photodimerization to give [5.6.4.6.5]-fused pentacycle **37** in 13% yield (72% starting material recovery) as a 13:1 mixture of diastereomers. The structure of cyanopentacycle **37** was unambiguously confirmed by analysis of a single crystal using X-ray diffraction. 5-Methoxycarbonyl indazole **38** also underwent photodimerization to cycloadduct **39** in 12% yield (72% starting material recovery) as a 3:1 mixture of diastereomers. In these cases, competitive excitation of these chromophores likely outcompetes the desired phototransposition resulting in this intriguing dearomative cycloaddition.

Our initial studies focused on substrates with non-removable substituents on N2 of the indazole core. However, we also recognized the potential value of *removable* substituents (i.e., protective groups) at this position. Several methodologies exist for N2-selective protection of indazoles (e.g., SEM-protection or THP-protection).[52–54] We investigated whether N2-protected indazoles would undergo phototransposition to give *N*-protected benzimidazoles, which could be deprotected to give protic benzimidazoles. This sequence would, therefore, constitute a formal transposition of protic 1H-indazoles to protic 1H-benzimidazoles.

We found that both SEM-protected 2H-indazole **40** and THP-protected 2H-indazole **42** underwent the transposition to give the corresponding products (protected benzimidazoles **41** and **43**) in

This article is protected by copyright. All rights reserved.

15213773, ja, Downloaded from https://onlinelibrary.wiley.com/doi/10.1002/anie.202423803 by Univ of California Lawrence Berkeley National Lab, Wiley Online Library on [02/03/2025]. See the Terms and Conditions (https://onlinelibrary.wiley.com/terms-and-conditions) on Wiley Online Library for rules of use; OA articles are governed by the applicable Creative Commons License

Accepted Manuscript

10.1002/anie.202423803

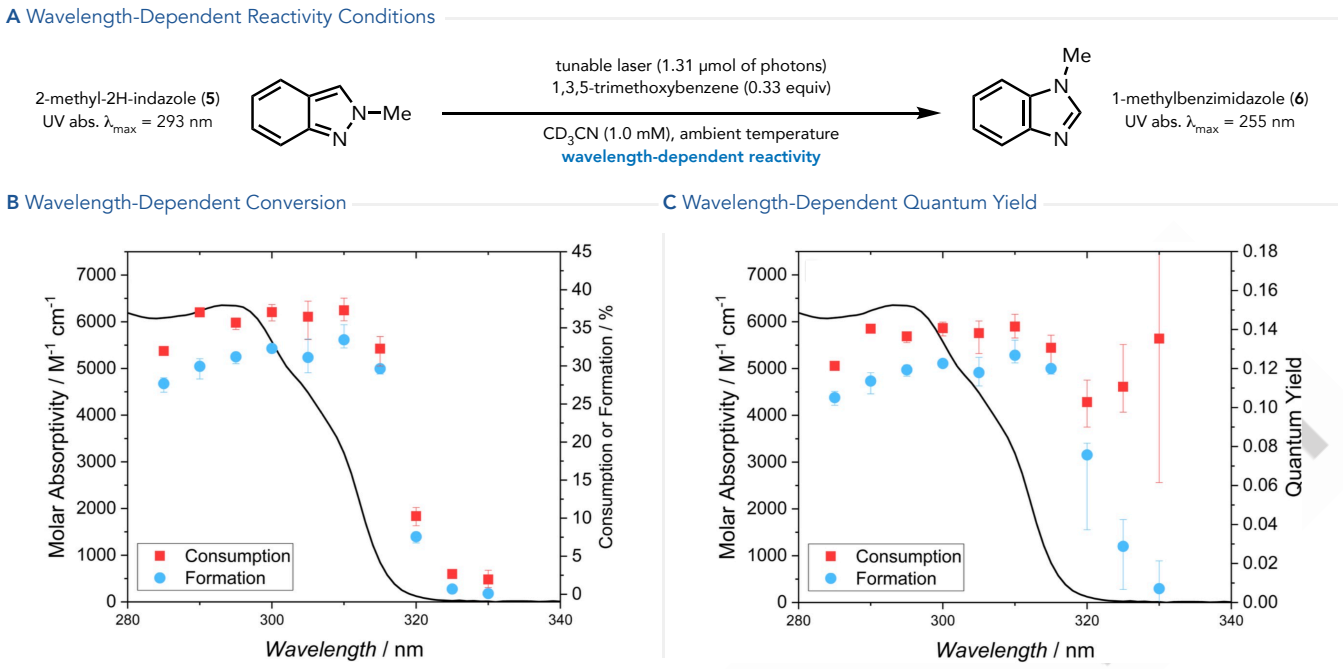

Figure 4. (a) Conditions for wavelength-dependent reactivity studies; (b) Photochemical action plot for 2-methylindazole phototransposition, plotting substrate consumption (red) and product formation (blue) against irradiation wavelength; (c) Phototransposition quantum yields of substrate consumption (red) and product formation (blue) plotted against irradiation wavelength. Error bars represent standard error for triplicate runs of each datapoint. For panels B and C, the absorption spectrum of the substrate – 2-methyl-2H-indazole – is plotted as a solid black line and molar absorptivity is given on the leftmost Y axis.

84% yield and 85% yield, respectively. A high yielding "one-pot" protocol for the transposition of 1H-indazole to an *N*-protected benzimidazole was achieved via the *in situ* generation of the SEM-protected 2H-tautomer (**40**, Figure 3H) giving the SEM-protected benzimidazole transposition product (**41**) in 57% yield with 11% remaining SEM-protected indazole after 24 h. The same *in situ* protection and irradiation strategy yielded THP-protected benzimidazole **43** in 59% yield with 13% remaining THP-protected indazole. SEM-protected and THP-protected benzimidazoles are known to undergo deprotection under Brønsted or Lewis acidic conditions,[55–57] and the former may also be deprotected by fluoride sources.[58]

With the scope of the transformation established, we turned our attention to characterizing the wavelength-dependent reactivity of this phototransposition. Given the enhanced photoreactivity of the indazole 2H-tautomer, we sought to gain insight as to whether the λ_{max} of the substrate matched that of the light source. The emission spectrum for the 310 nm light source – a Luzchem LZC-ORG photobox equipped with UVB-emitting white phosphor lamps – is shown in the Supporting Information. Comparing the UV–Vis absorption spectrum for 2-methylindazole (**5**, Figure 2A) and the emission spectrum reveals that substrate absorption is blueshifted relative to the emission spectrum of the light source, suggesting that the reaction may proceed most efficiently at wavelengths longer than the λ_{max} of the substrate. Notably, we found that the phototransposition even proceeds to a moderate degree when the substrate is irradiated with light centered at 350 nm (*vide supra*), which is not strongly absorbed by the 2-methylindazole model substrate (**5**, Figure 2A).

As there is increasing evidence that UV–Vis absorption spectra are not accurate predictors of wavelength-dependent reaction efficiency,[20,59,60] we generated a photochemical action plot for the phototransposition of 2-methylindazole (**5**) to give 1-methylbenzimidazole (**6**). First, we observed that the phototransposition occurs rapidly at a concentration of 1.0 mM in deuterated acetonitrile (CD_3CN) under ambient conditions when irradiated with a 305 nm beam from a tunable nanosecond pulsed laser. Specifically, 0.50 μmol of 2-methylindazole (**5**) was fully converted to 1-methylbenzimidazole (**6**) after approximately 5 min of irradiation, corresponding to the delivery of roughly one quintillion photons of 305 nm light.

We subsequently characterized the wavelength-dependent conversion of the phototransposition by quantifying both starting material consumption and product formation after irradiation with a constant number of photons at monochromatic wavelengths in 5 nm increments spanning 285–330 nm. Specifically, 1.31 μmol photons each at several monochromatic irradiation wavelengths were delivered to a series of identical reaction samples prepared from a stock solution of 1 mM 2-methylindazole (**5**) in CD_3CN. The consumption of **5** and formation of **6** were tracked by ^1H NMR spectroscopy in triplicate, and the photochemical action plot is shown in Figure 4B (refer to the Supporting Information for details). Under these experimental conditions, the conversion was indeed found to be consistently high even beyond the absorbance maximum, with product formation at or above 30% observed for excitation wavelengths up to 315 nm. Importantly, the absorbance of the product (1-methylbenzimidazole, **6**) becomes significant below 290 nm, which is likely reflected in the slight reduction in conversion at 285 nm due to an inner-filter effect. The action plot also revealed that trace undetermined side products appear to have a proportional formation at each excitation wavelength.

This article is protected by copyright. All rights reserved.

15213773, ja, Downloaded from https://onlinelibrary.wiley.com/doi/10.1002/anie.202423803 by Univ of California Lawrence Berkeley National Lab, Wiley Online Library on [02/03/2025]. See the Terms and Conditions (https://onlinelibrary.wiley.com/terms-and-conditions) on Wiley Online Library for rules of use; OA articles are governed by the applicable Creative Commons License

Accepted Manuscript

10.1002/anie.202423803

RESEARCH ARTICLE

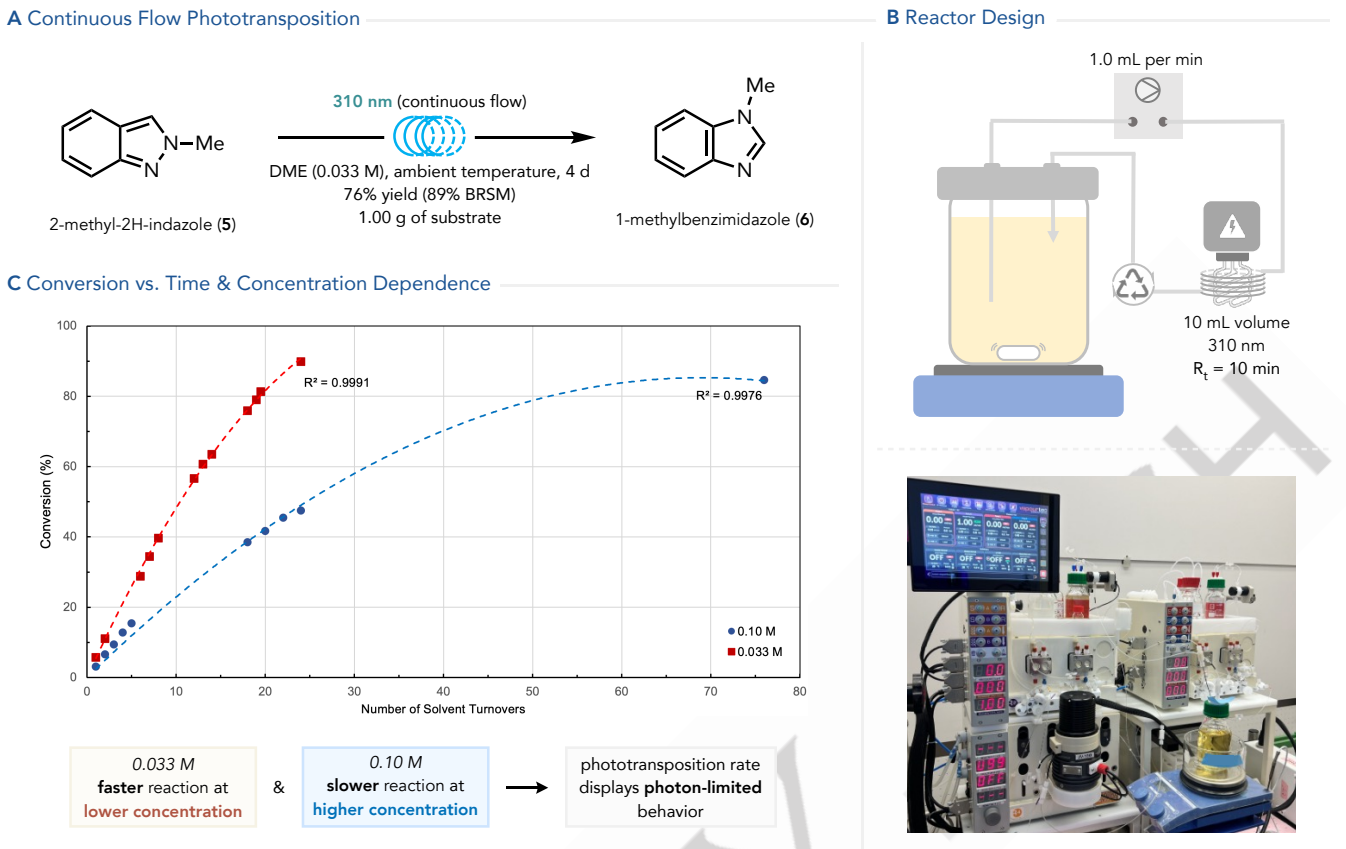

Figure 5. (a) Evaluation of phototransposition in flow without exclusion of air or trace water; (b) Photoflow reactor design; (c) Conversion with respect to solvent turnover number, where one solvent turnover is defined as the complete passage of the reaction mixture volume through the reactor, reflecting one cycle of exposure to the reaction conditions. Conversion tracked by UPLC and calculated as (% area number) / (% area number + % area number) at 268 nm.

To further investigate the efficiency of the reaction, the wavelength-dependent quantum yields were determined (Figure 4C; refer to the Supporting Information for details). The reaction displays a consistent and relatively high quantum yield of approximately 0.13 for wavelengths up to 315 nm. At longer wavelengths, low molar absorptivities and the accuracy of NMR spectroscopic quantification of conversion make quantum yields more challenging to assess under the experimental conditions. The error bars on the quantum yields beyond 320 nm (based on triplicate repeats) are an underestimate and it is possible that the quantum yields stay constant even beyond 320 nm. Nonetheless, these consistently high quantum yields at 1 mM substrate concentration allow for irradiation wavelengths longer than the absorbance maxima to be employed without sacrificing conversion efficiency, while benefiting from the enhanced penetration depth and lower energy usage that accompanies the use of these wavelengths.

Interestingly, the absorption spectrum of the product and minor side products displayed a significant absorbance tail into longer wavelengths. As these overlap with the starting material absorbance, they can therefore influence the reaction kinetics at each irradiation wavelength at higher conversions. This “inner filter effect” could, in part, explain the continuing high conversions at longer wavelengths (see the Supporting Information for details). In this specific case and under the examined conditions, the constant and high quantum yields – with the suggestion of a local maximum at 310 nm – over the examined wavelengths are most likely responsible for the redshifted action plot. These data underpin the notion that photons of longer wavelength and less energy can be equally efficient as photons of higher energy.

In general, it is likely that a variety of other factors contribute to the observed redshift of the photochemical action plots – and often times higher quantum efficiencies on the red-side of the absorption spectrum – with respect to substrate absorbance; this mismatch has been extensively studied by Barner-Kowollik and coworkers.[59] For example, irradiation with different wavelengths may promote the substrate to more productive excited states (e.g., states that lead to faster productive ISC) or to longer lived excited states (e.g., singlet vs. triplet), both of which could contribute to the observed redshift, in addition to the effects of potential vibrational coupling or absorbance of vibrationally “hot” substrates.[60]

Equipped with confirmation that the phototransposition proceeds efficiently using narrow-band irradiation centered at 310 nm as shown in Figure 4B, we sought to perform this reaction in flow on a large scale using a narrow-band 300–310 nm light source. The results from our continuous flow experiments are summarized in Figure 5. Our initial investigation was conducted on a 1.00 g scale with modified batch reaction conditions, utilizing a Vapourtec R-Series system equipped with a UV-150 photochemical flow reactor with fluoropolymer tubing (10 mL internal volume) and a 9 W, 310 nm low-pressure mercury lamp (Figure 5A). The reaction mixture, prepared at a concentration of 0.033 M in DME, was recirculated through the reactor at a flow rate of 1.0 mL/min, corresponding to a 10-min residence time. The reaction was

This article is protected by copyright. All rights reserved.

15213773, ja, Downloaded from https://onlinelibrary.wiley.com/doi/10.1002/anie.202423803 by Univ of California Lawrence Berkeley National Lab, Wiley Online Library on [02/03/2025]. See the Terms and Conditions (https://onlinelibrary.wiley.com/terms-and-conditions) on Wiley Online Library for rules of use; OA articles are governed by the applicable Creative Commons License

Accepted Manuscript

performed at ambient temperature with 99% light intensity. After 24 solvent turnovers, the process achieved 90% conversion, affording methylbenzimidazole **6** in an isolated yield of 76% (89% BRSM; Figure 5C).

A follow-up experiment was conducted to clarify the impact of concentration on conversion. Here, the reaction mixture was prepared at a concentration of 0.1 M in DME and subjected to the previously defined reaction conditions. At this higher substrate concentration, the photochemical reaction efficiency decreases; the reaction required over 70 solvent turnovers to achieve conversion above 80% as the "inner filter effect" is amplified. Additionally, the isolated yield was lower at 65% (79% BRSM) with a concomitant decrease in mass balance (83% at 0.1 M compared to 91% at 0.033 M) resulting from the formation of an insoluble, polymeric side product. Since the rate of phototransposition in terms of percent conversion was found to be inversely proportional to the reaction concentration as shown in Figure 5C, the reaction is likely to be photon limited (see the Supporting Information for details). Overall, this translational experiment showcases the utility of information derived from our wavelength-dependent reactivity analysis in a synthetically useful context.

Conclusion

We herein expand the scope of photomediated skeletal editing strategies by providing a detailed investigation of the wavelength-dependent transmutative phototransposition of 2H-indazoles to benzimidazoles. By identifying the enhanced photoreactivity of the 2H-tautomer, we optimized reaction conditions to achieve high yields under an operationally simple setup using UVB light, without the need for specialized air- or moisture-free environments. This work also highlights the impact of subtle electronic effects on the photoreactivity of indazole substrates, demonstrating that electron-rich N2 substituents and selective substitution at C3 enable productive transformations, while certain C5 and C6 substituents significantly diminish reactivity. Additionally, the development of *in situ* protection strategies to generate 2H-indazole tautomers further broadens the utility of this transformation for *N*-substituted benzimidazole synthesis. Our investigation also underscores the importance of leveraging photophysical insights to refine photochemical methods and the potential of wavelength-dependent strategies to selectively access pharmaceutically relevant heteroaromatic frameworks.

Acknowledgements

R.S. is grateful to the National Institute of General Medical Sciences (NIGMS R35 GM130345), Merck Sharp and Dohme LLC, a subsidiary of Merck & Co., Inc., Rahway, NJ, USA (MSD), and the National Science Foundation (NSF) under the Center for Computer-Assisted Synthesis (CCAS) for financial support (NSF CHE 2202693). G.L.B. thanks the National Science Foundation for support by the NSF Graduate Research Fellowship Program under Grant No. DGE 2146752. S.F.K. thanks the National Science Foundation for support by the NSF Graduate Research Fellowship Program under Grant No. DGE 1752814, as well as the National Institute of General Medical Sciences of the National Institutes of Health for support by the NIH F31 Fellowship under award number 1F31GM154485-01. C.B.-K. acknowledges the Australian Research Council (ARC) for funding in the context of two Discovery Grants (DP220100444 and DP230100445). The Central Analytical Research Facility (CARF) at QUT is gratefully acknowledged. Instruments in CoC-NMR are supported in part by National Institutes of Health (NIH S10OD024998). The CoC-MGCF was supported in part by NIH S10OD023532.

We thank Drs. Hasan Celik, Raynald Giovine, and the UC Berkeley Pines Magnetic Resonance Center's Core NMR Facility (PMRC Core) for spectroscopic assistance. We thank Dr. Nicholas Settineri (UC Berkeley) for X-ray crystallographic studies of **37**. We are grateful to Dr. Kathy Durkin and Dr. Dave Small for computational guidance. We thank Zhongrui Zhou and Ulla Anderson in the QB3/Department of Chemistry Mass Spectrometry Facility for accurate mass measurements.

Keywords: indazoles • photochemistry • rearrangements • wavelength dependence • photochemical action plots • continuous flow

References

[1] K. R. Campos, P. J. Coleman, J. C. Alvarez, S. D. Dreher, R. M. Garbaccio, N. K. Terrett, R. D. Tillyer, M. D. Truppo, E. R. Parmee, *Science* **2019**, *363*, 0805.

[2] J. Jurczyk, J. Woo, S. F. Kim, B. D. Dherange, R. Sarpong, M. D. Levin, *Nat. Synth* **2022**, *1*, 352–364.

[3] G. L. Bartholomew, F. Carpaneto, R. Sarpong, *J. Am. Chem. Soc.* **2022**, *144*, 22309–22315.

[4] B. D. Dherange, P. Q. Kelly, J. P. Liles, M. S. Sigman, M. D. Levin, *J. Am. Chem. Soc.* **2021**, *143*, 11337–11344.

[5] E. E. Hyland, P. Q. Kelly, A. M. McKillop, B. D. Dherange, M. D. Levin, *J. Am. Chem. Soc.* **2022**, *144*, 19258–19264.

[6] J. Woo, A. H. Christian, S. A. Burgess, Y. Jiang, U. F. Mansoor, M. D. Levin, *Science* **2022**, *376*, 527–532.

[7] J. C. Reisenbauer, O. Green, A. Franchino, P. Finkelstein, B. Morandi, *Science* **2022**, *377*, 1104–1109.

[8] B. J. H. Uhlenbruck, C. M. Josephitis, L. de Lescure, R. S. Paton, A. McNally, *Nature* **2024**, *631*, 87–93.

This article is protected by copyright. All rights reserved.

15213773, ja, Downloaded from https://onlinelibrary.wiley.com/doi/10.1002/anie.202423803 by Univ of California Lawrence Berkeley National Lab, Wiley Online Library on [02/03/2025]. See the Terms and Conditions (https://onlinelibrary.wiley.com/terms-and-conditions) on Wiley Online Library for rules of use; OA articles are governed by the applicable Creative Commons License

[9] G. L. Bartholomew, S. L. Kraus, L. J. Karas, F. Carpaneto, R. Bennett, M. S. Sigman, C. S. Yeung, R. Sarpong, *J. Am. Chem. Soc.* **2024**, *146*, 2950–2958.
[10] H. M. H. Nguyen, D. C. Thomas, M. A. Hart, K. R. Steenback, J. N. Levy, A. McNally, *J. Am. Chem. Soc.* **2024**, *146*, 2944–2949.
[11] Z. A. Tolchin, J. M. Smith, *J Am Chem Soc* **2024**, *146*, 2939–2943.
[12] D. Kim, J. You, D. H. Lee, H. Hong, D. Kim, Y. Park, *Science* **2024**, *386*, 99–105.
[13] J. Woo, C. Stein, A. H. Christian, M. D. Levin, *Nature* **2023**, *623*, 77–82.
[14] T. J. Pearson, R. Shimazumi, J. L. Driscoll, B. D. Dherange, D.-I. Park, M. D. Levin, *Science* **2023**, *381*, 1474–1479.
[15] B. Roure, M. Alonso, G. Lonardi, D. B. Yildiz, C. S. Buettner, T. dos Santos, Y. Xu, M. Bossart, V. Derdau, M. Méndez, J. Llaveria, A. Ruffoni, D. Leonori, *Nature* **2024**, 1–3.
[16] Q. Cheng, D. Bhattacharya, M. Haring, H. Cao, C. Mück-Lichtenfeld, A. Studer, *Nat Chem* **2024**, *16*, 741–748.
[17] Z. Wang, P. Xu, S.-M. Guo, C. G. Daniliuc, A. Studer, **2024**, DOI 10.26434/chemrxiv-2024-vtg73.
[18] A.-S. Paschke, Y. Brägger, B. Botlik, E. Staudinger, O. Green, B. Morandi, **2024**, DOI 10.26434/chemrxiv-2024-prwm8.
[19] J. Jurczyk, M. C. Lux, D. Adpressa, S. F. Kim, Y. Lam, C. S. Yeung, R. Sarpong, *Science* **2021**, *373*, 1004–1012.
[20] S. F. Kim, H. Schwarz, J. Jurczyk, B. R. Nebgen, H. Hendricks, H. Park, A. Radosevich, M. W. Zuerch, K. Harper, M. C. Lux, C. S. Yeung, R. Sarpong, *J. Am. Chem. Soc.* **2024**, *146*, 5580–5596.
[21] E. Boudry, F. Bourdreux, J. Marrot, X. Moreau, C. Ghiazza, *J. Am. Chem. Soc.* **2024**, *146*, 2845–2854.
[22] J. Luo, Q. Zhou, Z. Xu, K. N. Houk, K. Zheng, *J. Am. Chem. Soc.* **2024**, *146*, 21389–21400.
[23] J. W. Pavlik, in *Progress in Heterocyclic Chemistry* (Eds.: G.W. Gribble, J.A. Joule), Elsevier, **2003**, pp. 37–57.
[24] M. D'Auria, A. Guarnaccio, R. Racioppi, S. Stoia, L. Emanuele, in *Photochemistry of Heterocycles*, Elsevier, **2023**, pp. 91–160.
[25] C. Lefebvre, L. Fortier, N. Hoffmann, *European Journal of Organic Chemistry* **2020**, *2020*, 1393–1404.
[26] P. Beak, J. L. Miesel, W. R. Messer, *Tetrahedron Letters* **1967**, *8*, 5315–5318.
[27] H. Tiefenthaler, W. Dörscheln, H. Göth, H. Schmid, *Helvetica Chimica Acta* **1967**, *50*, 2244–2258.
[28] J. P. Ferris, K. V. Prabhu, R. L. Strong, *J. Am. Chem. Soc.* **1975**, *97*, 2835–2839.
[29] S. Wakamatsu, J. A. Barltrop, A. C. Day, *Chemistry Letters* **1982**, *11*, 667–670.
[30] W. Heinzelmann, M. Märky, P. Gilgen, *Helvetica Chimica Acta* **1976**, *59*, 1512–1527.
[31] R. E. Connors, J. W. Pavlik, D. S. Burns, E. M. Kurzweil, *J. Org. Chem.* **1991**, *56*, 6321–6326.
[32] M.-D. Su, *J. Phys. Chem. A* **2008**, *112*, 10420–10428.
[33] H. Wynberg, H. van Driel, *J. Am. Chem. Soc.* **1965**, *87*, 3998–4000.
[34] E. F. Ullman, B. Singh, *J. Am. Chem. Soc.* **1966**, *88*, 1844–1845.
[35] Hans. Wynberg, R. M. Kellogg, H. Van Driel, G. E. Beekhuis, *J. Am. Chem. Soc.* **1967**, *89*, 3501–3505.
[36] J. W. Pavlik, P. Tongcharoensirikul, K. M. French, *J. Org. Chem.* **1998**, *63*, 5592–5603.
[37] J. W. Pavlik, P. Tongcharoensirikul, *J. Org. Chem.* **2000**, *65*, 3626–3632.
[38] J. W. Pavlik, H. S. T. Martin, K. A. Lambert, J. A. Lowell, V. M. Tsefrikas, C. K. Eddins, N. Kebede, *Journal of Heterocyclic Chemistry* **2005**, *42*, 273–281.
[39] M.-D. Su, *J. Org. Chem.* **2009**, *74*, 6055–6063.
[40] R. C. F. Jones, A. Chatterley, R. Marty, W. M. Owton, M. R. J. Elsegood, *Chem. Commun.* **2014**, *51*, 1112–1115.
[41] M.-D. Su, *J. Phys. Chem. A* **2015**, *119*, 9666–9669.
[42] C. Bracken, M. Baumann, *Org. Lett.* **2023**, *25*, 6593–6597.
[43] C. M. Nunes, I. Reva, R. Fausto, *J. Org. Chem.* **2013**, *78*, 10657–10665.

This article is protected by copyright. All rights reserved.

15213773, ja, Downloaded from https://onlinelibrary.wiley.com/doi/10.1002/anie.202423803 by Univ of California Lawrence Berkeley National Lab, Wiley Online Library on [02/03/2025]. See the Terms and Conditions (https://onlinelibrary.wiley.com/terms-and-conditions) on Wiley Online Library for rules of use; OA articles are governed by the applicable Creative Commons License

Accepted Manuscript

10.1002/anie.202423803

[44] C. Bracken, M. Baumann, *J. Org. Chem.* **2020**, *85*, 2607–2617.
[45] F. Strieth-Kalthoff, M. J. James, M. Teders, L. Pitzer, F. Glorius, *Chem. Soc. Rev.* **2018**, *47*, 7190–7202.
[46] J. P. Ferris, F. R. Antonucci, *J. Am. Chem. Soc.* **1974**, *96*, 2010–2014.
[47] A. N. Nesmeyanov, E. B. Zavelovich, V. N. Babin, N. S. Kochetkova, E. I. Fedin, *Tetrahedron* **1975**, *31*, 1463–1464.
[48] M. Noda, N. Hirota, M. Sumitani, K. Yoshihara, *J. Phys. Chem.* **1985**, *89*, 399–401.
[49] V. Rousseau, H. G. Lindwall, *J. Am. Chem. Soc.* **1950**, *72*, 3047–3051.
[50] M. Cheung, A. Boloor, J. A. Stafford, *J. Org. Chem.* **2003**, *68*, 4093–4095.
[51] S. R. Baddam, N. Uday Kumar, A. Panasa Reddy, R. Bandichhor, *Tetrahedron Letters* **2013**, *54*, 1661–1663.
[52] G. Luo, L. Chen, G. Dubowchik, *J Org Chem* **2006**, *71*, 5392–5395.
[53] D. J. Slade, N. F. Pelz, W. Bodnar, J. W. Lampe, P. S. Watson, *J. Org. Chem.* **2009**, *74*, 6331–6334.
[54] Y. Zhan, X. Ding, H. Wang, H. Yu, F. Ren, *Tetrahedron Letters* **2018**, *59*, 2150–2153.
[55] A. M. Palmer, V. Chiesa, A. Schmid, G. Münch, B. Grobbel, P. J. Zimmermann, C. Brehm, W. Buhr, W.-A. Simon, W. Kromer, S. Postius, J. Volz, D. Hess, *J. Med. Chem.* **2010**, *53*, 3645–3674.
[56] S. Wang, V. Tsui, T. D. Crawford, J. E. Audia, D. J. Burdick, M. H. Beresini, A. Côté, R. Cummings, M. Duplessis, E. M. Flynn, M. C. Hewitt, H.-R. Huang, H. Jayaram, Y. Jiang, S. Joshi, J. Murray, C. G. Nasveschuk, E. Pardo, F. Poy, F. A. Romero, Y. Tang, A. M. Taylor, J. Wang, Z. Xu, L. E. Zawadzke, X. Zhu, B. K. Albrecht, S. R. Magnuson, S. Bellon, A. G. Cochran, *J. Med. Chem.* **2018**, *61*, 9301–9315.
[57] J.-C. Carry, F. Clerc, H. Minoux, L. Schio, J. Mauger, A. Nair, E. Parmantier, R. Le Moigne, C. Delorme, J.-P. Nicolas, A. Krick, P.-Y. Abécassis, V. Crocq-Stuerga, S. Pouzieux, L. Delarbre, S. Maignan, T. Bertrand, K. Bjergarde, N. Ma, S. Lachaud, H. Guizani, R. Lebel, G. Doerflinger, S. Monget, S. Perron, F. Gasse, O. Angouillant-Boniface, B. Filoche-Rommé, M. Murer, S. Gontier, C. Prévost, M.-L. Monteiro, C. Combeau, *J. Med. Chem.* **2015**, *58*, 362–375.
[58] T. Murata, Y. Yamamoto, Y. Yakiyama, K. Nakasuji, Y. Morita, *Bulletin of the Chemical Society of Japan* **2013**, *86*, 927–939.
[59] I. M. Irshadeen, S. L. Walden, M. Wegener, V. X. Truong, H. Frisch, J. P. Blinco, C. Barner-Kowollik, *J. Am. Chem. Soc.* **2021**, *143*, 21113–21126.
[60] S. L. Walden, J. A. Carroll, A.-N. Unterreiner, C. Barner-Kowollik, *Advanced Science* **2024**, *11*, 2306014.

This article is protected by copyright. All rights reserved.

15213773, ja, Downloaded from https://onlinelibrary.wiley.com/doi/10.1002/anie.202423803 by Univ of California Lawrence Berkeley National Lab, Wiley Online Library on [02/03/2025]. See the Terms and Conditions (https://onlinelibrary.wiley.com/terms-and-conditions) on Wiley Online Library for rules of use; OA articles are governed by the applicable Creative Commons License

Accepted Manuscript

10.1002/anie.202423803

WILEY VCH

RESEARCH ARTICLE

Entry for the Table of Contents

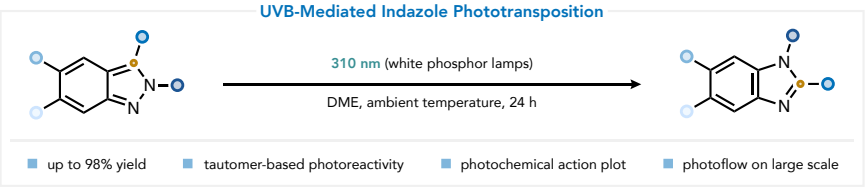

Several N2-substituted indazole derivatives efficiently undergo photorearrangement to benzimidazoles with UVB irradiation. Motivated by the difference between the wavelength at which the phototransposition is most efficient and the substrate absorbance λ_{max}, a photochemical action plot was constructed. Wavelength-dependent quantum yields were measured, and a photoflow protocol was established to perform the phototransposition on preparative scale.

Institute and/or researcher Twitter usernames: G. Logan Bartholomew: @gloganb, Sojung F. Kim: @SojungKim20, Federica Sbordone: @federica_sb, Joshua A. Carroll: @LaserJCarroll, Justin E. Jurczyk: @JustinJurczyk, Charles S. Yeung: @Charles_chem, Christopher Barner-Kowollik: @BarnerKowollik, Richmond Sarpong (group Twitter account): @SarpongGroup, University of California – Berkeley: @UCBerkeley

This article is protected by copyright. All rights reserved.

15213773, ja, Downloaded from https://onlinelibrary.wiley.com/doi/10.1002/anie.202423803 by Univ of California Lawrence Berkeley National Lab, Wiley Online Library on [02/03/2025]. See the Terms and Conditions (https://onlinelibrary.wiley.com/terms-and-conditions) on Wiley Online Library for rules of use; OA articles are governed by the applicable Creative Commons License

Accepted Manuscript